Journal of Ginseng Research 49 (2025) 42–52

Contents lists available at ScienceDirect

Journal of Ginseng Research

journal homepage: www.sciencedirect.com/journal/journal-of-ginseng-research

Research Article

Ginsenoside Rc prevents dexamethasone-induced muscle atrophy and enhances muscle strength and motor function

Aeyung Kim [a,*,1], Sang-Min Park [b,1], No Soo Kim [c], Musun Park [d], Seongwon Cha [d]

[a] Korean Medicine (KM) Application Center, Korea Institute of Oriental Medicine, Daegu, Republic of Korea
[b] College of Pharmacy, Chungnam National University, Daejeon, Republic of Korea
[c] KM Science Research Division, Korea Institute of Oriental Medicine, Daejeon, Republic of Korea
[d] KM Data Division, Korea Institute of Oriental Medicine, Daejeon, Republic of Korea

ARTICLE INFO

Keywords:
Dexamethasone
Ginsenoside Rc
Muscle atrophy
Muscle function
Skeletal muscle

ABSTRACT

Background: A decline in muscle mass and function can impact the health, disease vulnerability, and mortality of older adults. Prolonged use of high doses of glucocorticoids, such as dexamethasone (DEX), can cause muscle wasting and reduced strength. Ginsenoside Rc (gRc) has been shown to protect muscles by activating the PGC-1α pathway and improving mitochondrial function. The effects of gRc on muscle atrophy and function in mice are not fully understood.

Methods and results: The study discovered that gRc prevented the DEX-induced decrease in viability of C2C12 myoblasts and myotubes. Furthermore, gRc inhibited myotube degradation and the upregulation of muscle degradation proteins induced by DEX. Transcriptome analysis of myotubes showed that gRc enhances muscle generation processes while suppressing the TGF-β pathway and oxidative stress response. In mice, gRc effectively reversed the reductions in body weight, muscle mass, and muscle fibers caused by DEX. Furthermore, gRc significantly enhanced muscle strength and exercise capacity. Docking and transcriptome analyses indicated that gRc may act as a competitive inhibitor of DEX at the glucocorticoid receptor, potentially preventing muscle loss.

Conclusion: The study suggests that gRc can prevent DEX-induced muscle wasting and weakness. Consequently, it may be a viable treatment option for sarcopenia and muscle-related disorders in various medical conditions.

1. Introduction

In sarcopenia, muscle mass, strength, and function decline with age. Sarcopenia affects approximately 20 % of individuals aged 60 and older, and over 60 % of those aged 80 and above [1]. Hormonal changes, reduced mitochondrial function, inflammation, chronic diseases, and medications all contribute to sarcopenia [1–3]. As muscles weaken, maintaining independence becomes more challenging. The risks of osteoporosis and fractures increase, leading to a harmful cycle of prolonged hospital stays, reduced physical activity, and diminished muscle function. This not only reduces the quality of life in old age but also increases the risk of death. Therefore, enhancing muscle mass, strength, and function is essential for preventing and managing sarcopenia [4–6].

Synthetic glucocorticoids (GCs) like as dexamethasone (DEX) frequently commonly to treat different various medical conditions [7–9]. Prolonged or high-dose use can elevate myostatin, Atrogin1, MuRF1, and E3 ubiquitin ligase levels, causing muscle atrophy and strength reduction [10,11]. Furthermore, GCs increase the production of reactive oxygen species (ROS), impairing mitochondrial function and promoting muscle deterioration [12–15]. Therefore, therapeutic strategies that reduce GC-induced muscle atrophy have important clinical implications [11,16].

Ginseng root, scientifically known as Panax ginseng Meyer, is a popular herbal remedy with a long history of use in Asian cultures [17]. Ginseng contains numerous active components, including over 100 ginsenosides, with the majority being glycosylated ginsenosides like Rb1, Rb2, Rc, Rd, Re, and Rg1 [18]. Ginsenosides possess diverse pharmacological properties, including reducing oxidative stress, cancer, diabetes, and inflammation, and promoting vasorelaxation [19–21]. Several ginsenosides improve muscle strength and prevent muscle degradation [22]. In a previous study, we showed that ginsenoside Rc (gRc) can inhibit oxidative stress and enhance mitochondrial function

* Corresponding author. Korean Medicine (KM) Application Center, Korea Institute of Oriental Medicine, Daegu, 41062, Republic of Korea.
E-mail address: aykim71@kiom.re.kr (A. Kim).
[1] These authors have contributed equally to this work.

https://doi.org/10.1016/j.jgr.2024.09.002
Received 30 March 2024; Received in revised form 20 August 2024; Accepted 5 September 2024
Available online 11 September 2024

by activating the PGC-1α pathway in C2C12 murine muscle cells. Furthermore, gRc effectively inhibited myotube degradation and myoblast apoptosis induced by oxidative stress. This strongly suggests that gRc may be beneficial for treating weakness and muscle atrophy [23]. In this study, we investigated whether gRc can reduce DEX-induced muscle atrophy and improve muscle strength and function in both *in vivo* and *in vitro* setting. We analyzed muscle cell gene expression profiles and conducted molecular docking studies to understand the mechanism of action of gRc in DEX-induced muscle atrophy.

2. Materials and methods

2.1. C2C12 myoblast cell culture and myotube formation

The C2C12 myoblast cell line (CRL-1772) was obtained from the American Type Culture Collection (ATCC, Manassas, VA, USA) and grown in the growth medium (GM), Dulbecco's Modified Eagle Medium containing 4.5 g/L glucose (DMEM), along with 10 % heat-inactivated fetal bovine serum (FBS) and penicillin/streptomycin (P/S). To induce myotube formation, C2C12 myoblasts were cultured until reaching confluency in GM, followed by replacement of GM with differentiation medium (DM, DMEM with 2 % horse serum (HS) and P/S). The DM was replaced every 2 days for a period of 5–7 days. The cells were cultured at a temperature of 37 °C in a humidified incubator with 5 % CO2. DMEM, FBS, HS, and P/S were all acquired from Thermo Fisher Scientific (Waltham, MA, USA).

2.2. Chemicals

gRc (PHL89210, ≥90 % purity), DEX (D4902), dimethyl sulfoxide (DMSO; D8418), DEX-water soluble (D2915), resveratrol (Rv, R5010), 4',6-diamidino-2-phenylindole (DAPI, D8417), sodium dodecyl sulfate (SDS, L3771), methanol (#179337), carboxymethylcellulose (CMC; D5678), avertin (T48402), and 10 % formalin solution (HT5012) were all obtained from Sigma-Aldrich (St Louis, MO, USA. Neutralized 4 % paraformaldehyde (PFA) solution (PC2031-100-00) was acquired from Biosesang (Seongnam, Republic of Korea). gRc was dissolved in 100 % DMSO (20 mM stock) and stored at −20 °C.

2.3. Assays for cytotoxicity in myoblasts and myotubes

To evaluate the cytotoxic effects on myoblasts, a total of 5000 cells were seeded in each well of a 96-well culture plate. The cells were allowed to grow overnight and subsequently exposed to gRc, DEX, or a vehicle solution containing 0.1 % DMSO for 24 h. The cell viability was assessed using the EZ-Cytox Enhanced Cell Viability Assay Kit (Daeil Lab Service Co., Ltd., Seoul, Republic of Korea) and a SpectraMax3 microplate reader (Molecular Devices, LLC, Sunnyvale, CA, USA). To assess the cytotoxic effects on myotubes, cells differentiated for 5 days (referred to as DD5) were treated with gRc, DEX, or a vehicle for 24−48 h. Following treatment, the cells were stained with a crystal violet solution (0.2 % crystal violet in 20 % methanol) and quantified as described previously [23]. To examine the influence of gRc on DEX stimulation, the cells were pretreated with gRc for 12 h, and then treated with DEX.

2.4. Immunoblotting analysis

Whole cell lysates were extracted using the M-PER Mammalian Protein Extraction Reagent (#78501, Thermo Fisher Scientific). Muscle tissues were homogenized using the T-PER Tissue Protein Extraction Reagent (#78510; Thermo Fisher Scientific) and PreCellys instrument (Bertin Instruments, Montigny-le-Bretonneux, France). After determining the protein concentration using bicinchoninic acid assay (#23227; Thermo Fisher Scientific), proteins (25 μg per lane) were subjected to immunoblotting as described previously [23]. Protein levels were quantified using ImageJ software (National Institute of Health, USA), and the relative intensities of bands calculated after normalization to the β-actin value. Anti-myosin heavy chain (MyHC, MAB4470) and anti-muscle atrophy F-box (MAFbx/Atrogin1, ab168371) antibodies were obtained from R&D Systems (Minneapolis, MN, USA) and Abcam (Cambridge, UK), respectively. Antibodies against muscle ring-finger protein-1 (MuRF1, sc-398608) and β-actin (sc-47778) were acquired from Santa Cruz Biotechnology (Santa Cruz, CA, USA). Horseradish peroxidase (HRP)-conjugated anti-mouse IgG (#7076) and anti-rabbit IgG (#7074) were obtained from Cell Signaling Technology (Beverly, MA, USA).

2.5. Immunofluorescence staining for myosin heavy chain (MyHC)

The DD5 myotubes that were differentiated on glass bottom dishes (SPL Life Sciences, Pocheon, Republic of Korea) were pretreated with gRc for 12 h, subsequently exposed to 200 μM DEX for 48 h. Then, cells were subjected to immunofluorescence staining for MHC as described previously [23]. The fusion index and myotube length were evaluated in ten representative images per group using ImageJ software. The fusion index was calculated by dividing the number of nuclei in multinucleated cells by the total number of nuclei, and then multiplying by 100.

2.6. Dexamethasone-induced muscle atrophy experiments using C57BL/6N mice

Eight-week-old male C57BL/6N mice (OrientBio, Seongnam, Republic of Korea) with an average body weight of 22–24 g were housed in a specific pathogen-free animal laboratory facility with controlled conditions (22 ± 2 °C, 45 ± 10 % humidity, and a 12-h light-dark cycle). After 7 days, the mice were divided into five groups (n = 10 per group). Water-soluble DEX was dissolved in sterile PBS, while gRc and Rv were resuspended in sterile 0.5 % CMC in PBS. Starting from day 1 (D1), mice were administered daily intraperitoneal (i.p.) injections of PBS (Group 1, normal control) or 25 mg/kg DEX (Groups 2–5) to induce muscle atrophy, as per established protocol [24,25]. After 30 min, the mice received daily oral administration of gRc at 5 mg/kg (Group 3) or 10 mg/kg (Group 4). The positive control group (Group 5) received Rv (150 mg/kg) [25], and Groups 1 and 2 received PBS instead of gRc. The mice were weighed every day for 10 days. On day 11 (D11), mice were euthanized through i.p. injection of 2 % avertin in PBS (240 mg/kg). The gastrocnemius (GA), soleus (SO), and tibialis anterior (TA) muscle tissues were removed, weighed, snap-frozen on dry ice, and then stored at −80 °C. Experimental procedures were reviewed and approved by the Institutional Animal Care and Use Committee of the Korea Institute of Oriental Medicine (approval No: 22–068; approval Date: July 27, 2022). Animal studies were carried out in compliance with the regulations outlined in the Care and Use of Laboratory Animals guidelines established by the Ministry of Food and Drug Safety in the Republic of Korea.

2.7. Grip strength test and rotarod test

The maximal peak grip strength and coordinated muscle activity of mice were evaluated using a digital grip strength meter (DJ-356; Daejong Instrument Industry Co., Seoul, Republic of Korea) and a rotarod instrument (ROTA-ROD, B.S Technolab INC, Seoul, Republic of Korea) according to the established protocol [26].

2.8. Histological analysis of muscle tissues

PFA-fixed skeletal muscles were embedded in the Tissue-Tek OCT Compound (#4583; Kakura Finetek, Torrance, CA, USA). Muscle slices with a thickness of 10 μm were prepared on a positively charged microscope slide and stained with hematoxylin and eosin (H&E). At a magnification of 20 × , digital images were obtained, and cross-sectional areas (CSAs) of at least 100 muscle fibers were quantitatively measured

using ImageJ with a cross-sectional analyzer plugin.

2.9. Acquisition and preprocessing of RNA sequencing data

Total RNA (over 1 μg) was extracted from C2C12 myotubes using Maxwell method (Promega). The mRNA sequencing libraries were prepared with the MGIEasy RNA Directional Library Prep kit (#1000006386; MGI Tech, Shenzhen, China). The cDNA was then prepared for sequencing by adding 'A' bases, ligating adapters, and performing PCR enrichment. The library was quantified using QauntiFluor ONE dsDNA System (Promega), followed by circularization, digestion, and cleanup. DNA nanoballs (DNB) were quantified by QauntiFluor ssDNA System (Promega) and sequenced on the MGIseq system (MGI) with 100 bp paired-end reads. The quality of sequencing reads was assessed using FastQC (v0.11.9). The MGISEQ adapter sequences and low-quality base pairs were removed using TrimGalore (v0.6.6). The trimmed reads were then aligned to the mouse reference genome (GRCm39) using STAR (v2.7.9a) with default settings [27]. Expression levels, such as expected read count or transcript per million (TPM) per gene, were quantified using RSEM (v1.3.3) along with the GRCm39.104 gene annotation [28].

2.10. Differential gene expression and functional enrichment analysis

In C2C12 myotube samples, a Wald test statistic implemented in DESeq2 package in R was employed to measure the degree of differential expression in the two groups for each gene, providing a $\log_2$ fold-change, *p*-value, adjusted *p*-value [29]. Subsequently, gene set enrichment analysis (GSEA) was performed on all genes, ranked by their Wald test statistics [30]. GSEA utilizes well-curated gene sets, those available from the MSigDB (https://www.gsea-msigdb.org/gsea/msigdb), to identify biological pathways significantly enriched with genes exhibiting altered expression between groups.

2.11. Molecular docking analysis

The chemical structures of DEX were collected from the PubChem database [31]. Since the 3D structure of gRc is not provided in the PubChem database, we used the 3D sdf structure information provided by the Human Metabolome Database [32]. The structural and functional information of the glucocorticoid receptor (GR, entry number: P04150, Gene Symbol: NR3C1) was verified in the UniProt database [33]. Additionally, the 3d sdf structure information of GR was collected from the AlphaFold 2.0 database [34]. DEX, gRc and GR were converted to PDBQT file format using OpenBabel software (v3.1.1) [35]. Binding affinity calculations from molecular docking were performed using AutoDock Vina (v4.2.6) [36], and the parameters were set as follows: exhaustiveness = 100; center = [0, 0, 0], box size = [126,126,126]. All other variables used default settings. In the docking analysis of GR and DEX, three prediction results with low binding affinity were visualized, and in the docking analysis of GR and gRc, one case with the lowest binding affinity was visualized. 3D secondary structures and 2D diagrams were visualized using Discovery Studio Visualizer (v21.1.0.20), and 3D molecular surfaces to find interacting pores were visualized using AutoDockTools (v1.5.6). The nuclear receptor (NR) ligand-binding domain (LBD) of GR was searched in the UniProt Database and compared with the interaction sites in the visualized data.

2.12. Statistical analysis

The data was analyzed using R software version 4.2.2 and GraphPad Prism 9.5.1. (GraphPad Software, San Diego, CA, USA). The data values are shown as the means with standard error of the mean (SEM) from several experiments. The variance in group comparisons was assessed through one-way analysis of variance (ANOVA) and subsequently verified using Dunnett's multiple comparison test. Statistical significance was determined at a threshold of $p < 0.05$.

3. Results

3.1. gRc alleviates DEX-induced cytotoxicity in C2C12 myoblasts and myotubes

Fig. 1A shows the chemical structure of gRc. To examine the protective effects of gRc on muscle cells, we first determined the viability of C2C12 myoblasts and myotubes after gRc and DEX. At concentrations up to 20 μM, gRc did not show any cytotoxic effects on myoblasts or myotubes. Instead, it slightly increased their viability, consistent with previous findings [23]. In addition, 0.1 % DMSO (vehicle) had no effect on cell viability or morphology (Fig. 1B). As previously reported [25], DEX at 200 μM decreased the viability of myoblast and myotube by approximately 45 % and 35 %, respectively (Fig. 1C). Therefore, we used 200 μM DEX to induce cell damage and gRc concentrations of up to 20 μM to assess its protective effect. As shown in Fig. 1D, DEX significantly inhibited myoblast proliferation and induced myotube degradation. However, cells pretreated with gRc recovered from DEX-induced damage to levels similar to those of the control cells. Cell viability analysis showed that gRc significantly increased the viability of myoblasts and myotubes (Fig. 1E).

3.2. gRc inhibits DEX-induced degradation of C2C12 myotubes

We assessed gRc's potential protective properties against DEX-induced muscle atrophy in C2C12 myotubes. As depicted in Fig. 2A, immunofluorescence staining confirmed high MyHC levels in normal myotubes, with the majority containing more than 10 nuclei. The decrease in MyHC expression caused by DEX was mitigated by pretreatment with gRc, maintaining levels similar to control myotubes. Control myotubes usually exhibit a fusion index of approximately 70 %. However, the DEX reduced it by 40 % and decreased myotube length by approximately 77 %. Pretreatment with gRc maintained the fusion index similar to control myotubes and preserved myotube length at 70–87 % of the control length, even with DEX treatment (Fig. 2B and C). Immunoblotting analysis showed that DEX significantly reduced MyHC expression and increased levels of the muscle-degrading proteins Atrogin-1 and MuRF1. Pretreatment with gRc effectively reduced the DEX-induced decrease in MyHC and increase in Atrogin-1 and MuRF1 expression (Fig. 2D).

3.3. gRc reverses the muscle atrophy-related pathways activated by DEX

To explore how gRc protects against DEX-induced muscle atrophy in C2C12 myotubes, we analyzed RNA-Seq data from DEX-treated C2C12 myotubes with and without gRc pretreatment. Differential gene expression analysis showed a dose-dependent effect, with higher gRc leading to more significant changes in gene expression (Fig. 3A). GSEA showed that gRc significantly improved protection against DEX-induced muscle atrophy at the pathway level (Fig. 3B and C). Pretreatment with gRc increased the expression of genes related to muscle development, including those involved in myogenesis, the mTORC1 signaling pathway, and PGC-1α and ERRα target genes. Conversely, gRc suppressed genes linked to the TGF-β signaling pathway, which hinders muscle development. Furthermore, it seemed to safeguard muscle cells by reducing the apoptotic signaling pathway and oxidative stress response. gRc significantly increased the expression of genes related to mitochondrial function, such as the mitochondrial membrane protein complex, cellular respiration, oxidative phosphorylation, energy production, and ATP synthesis. Additionally, we compared the pathways affected by gRc under DEX-induced and H_2O_2-induced conditions, as detailed in our previous study [23], to further investigate its common protective mechanisms (Supplementary Fig. S1A). Despite different stressors, gRc consistently boosted pathways related to mitochondrial

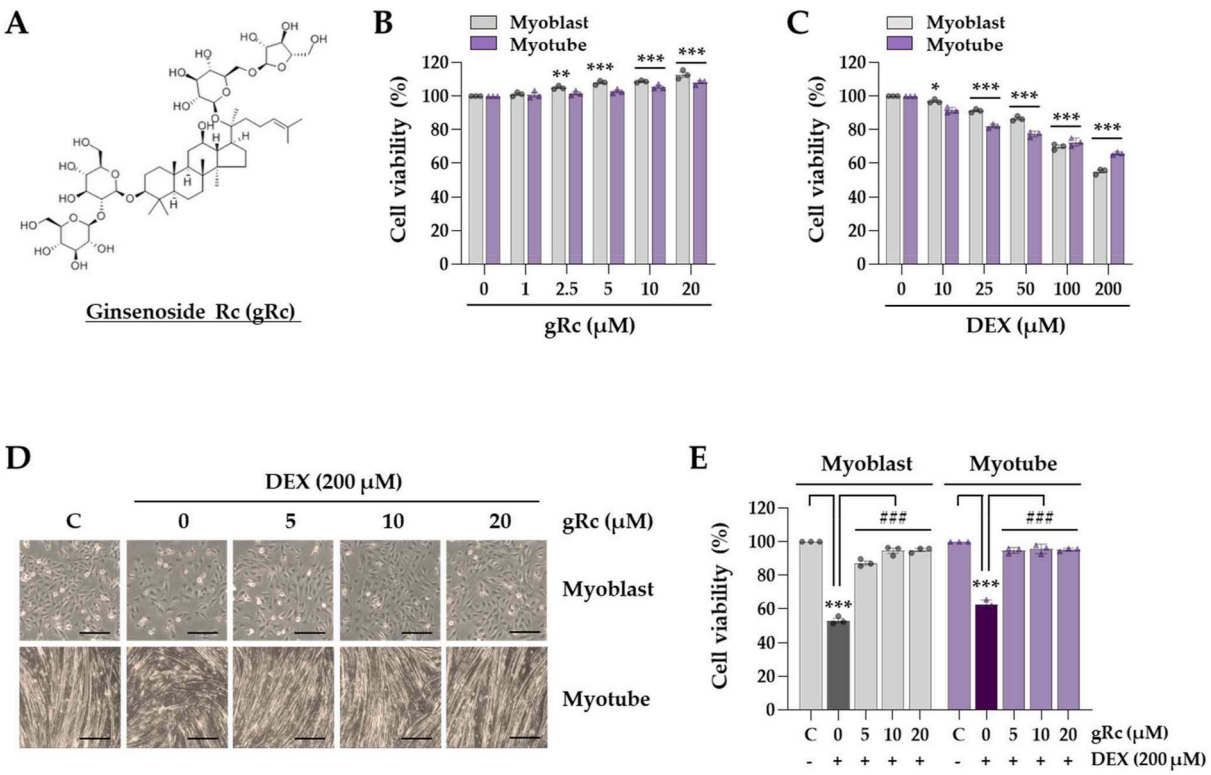

Fig. 1. Effects of gRc on the cytotoxic effects induced by DEX in C2C12 myoblasts and myotubes. (A) The chemical structure of ginsenoside Rc (gRc). (B, C) Myoblasts or myotubes were treated with gRc (B) or DEX (C). Relative cell viability was presented as the means ± SEM (n = 3). (D, E) Myoblasts or myotubes pretreated with gRc were incubated with DEX. Changes in cell morphology were observed under an inverted microscope (D), and the relative cell viability was expressed as the means ± SEM (n = 3) (E). Scale bar = 100 μm *$p < 0.05$, **$p < 0.01$, ***$p < 0.001$ vs. vehicle-treated cells, ###$p < 0.001$ vs. DEX + vehicle-treated cells.

function, oxidative phosphorylation, and ATP synthesis in both conditions (Supplementary Fig. S1B). Furthermore, gRc consistently reduced apoptotic signaling and TGF-β signaling pathways in both models (Supplementary Figs. S1B and S1C). These findings suggest that the core mechanisms by which gRc exerts its muscle-protective effects are preserved regardless of the specific type of stress encountered. Within these pathways, gRc significantly upregulated the expressions of several genes, including *Ak4* (adenylate kinase 4), *BNIP3* (Bcl-2 interacting protein 3), *Ckmt2* (mitochondrial creatine kinase), and *Mb* (myoglobin) (Supplementary Fig. S2).

3.4. Oral administration of gRc improves body weight, grip strength, and motor function in mice with DEX-induced muscle atrophy

To investigate the effect of gRc on DEX-induced muscle atrophy, a group of 8-week-old male C57BL/6 mice were subjected to intraperitoneal injections of DEX. Following this, the mice were administered with either gRc or Rv for a duration of 10 days (Fig. 4). The mice in Group 2 (DEX + vehicle) showed a gradual body weight loss throughout the experiment, similar to previous studies [15,25]. In Group 3 (DEX + 5 mg/kg gRc), body weight slightly increased compared to Group 2 until day 5, but not after that. The Group 4 (DEX +10 mg/kg gRc) and Group 5 (DEX + 150 mg/kg Rv) exhibited significantly reduced weight loss compared to Group 2 throughout the experiment (Fig. 4B). After the DEX injection, there was a notable 8.5 % decrease in body weight over time. The weight loss caused by DEX was restored by 4.6 % and 5.6 % after treatment with gRc (10 mg/kg) and Rv (150 mg/kg), respectively (Fig. 4C). To evaluate the impact of gRc on muscle strength, grip strength on day 9 was analyzed. The Group 2 exhibited a notable decline in grip strength, around 40.8 % lower than Group 1. The decrease in grip strength induced by DEX was fully reversed in the groups treated with gRc and Rv, restoring their grip strength to the level of control mice (Fig. 4D). To evaluate the impact of gRc on motor coordination, the rotarod test was conducted on day 10. Repeated DEX injections significantly reduced motor coordination, leading to a 50 % shorter stay on the rotarod (82.57 s) compared to control mice (164.40 s). Conversely, mice given 5 and 10 mg/kg gRc showed improved motor coordination, achieving 93.3 % (153.41s) and 79.99 % (131.5 s), respectively, compared to controls. The group treated with Rv showed a recovery rate of 91.9 % (151.10 s) compared to the control value (Fig. 4E). The two behavioral assessments provide strong evidence that gRc has the potential to mitigate muscular dysfunction caused by DEX in experimental mice.

3.5. Oral administration of gRc reduces muscle loss, atrophy, and degradation caused by DEX injection

Considering that DEX-induced muscle dysfunction was alleviated by gRc administration, we further investigated whether this effect was associated with the inhibition of muscle loss and muscle atrophy. On the 11th day, the weights of GA, SO, and TA muscles were measured, and their diameters were recorded. Supplementary Fig. S3 displays representative photographs of muscle tissues. DEX reduced the weight and diameter of the GA, SO, and TA. After administering gRc and Rv to DEX-treated mice, there were slight increases in the weights of all three muscles (Fig. 4F). In addition, gRc and Rv mitigated the DEX-induced decrease in muscle diameter, with the most significant impact in the GA (Fig. 4G). Muscle sections were stained with H&E to assess the impact of gRc on myofiber size, and CSA was measured using a standard protocol [25,37]. Representative images of cross-sectional myofibers are displayed in Fig. 5A. The DEX group showed reductions of approximately 32.0 %, 28.6 %, and 42.2 % in the mean CSA of the GA, SO, and

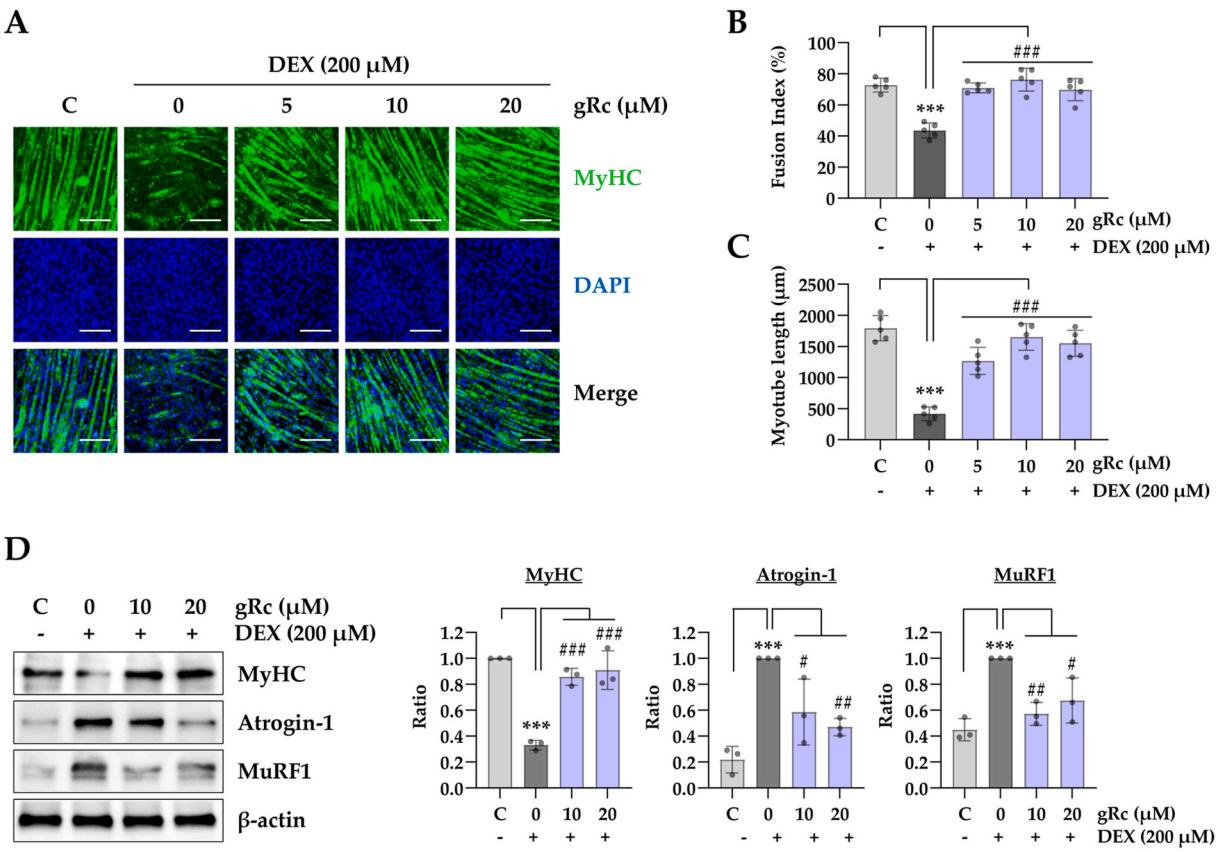

Fig. 2. Effects of gRc on DEX-induced myotube degradation. (A) Myotubes pretreated with gRc were treated with DEX, and then stained for MyHC (green) and nuclei (blue). Scale bar = 200 μm. The fusion index (B) and myotube length (C) were presented as the mean ± SEM (n = 7). (D) The protein levels of MyHC, Atrogin-1, and MuRF1 in myotubes were determined by Immunoblotting. ***$p < 0.001$ vs. vehicle-treated cells, #$p < 0.05$, ##$p < 0.01$, ###$p < 0.001$ vs. DEX + vehicle-treated cells.

TA, respectively, compared to the control group. The administration of 10 mg/kg gRc restored the CSA of the GA, SO, and TA to 84.4 %, 90.8 %, and 76.8 % of the controls, respectively. The administration of Rv restored the CSA of GA, SO, and TA to 103.1 %, 91.8 %, and 78.9 % of the control levels, respectively (Fig. 5B). In the control group, the frequency of CSA distribution was around 25.8 % for the range of 200–600 μm^2 and 74.2 % for the range of 600–2000 μm^2 (Fig. 5C, Supplementary Fig. S4). After DEX injection, the proportions changed to approximately 52.2 % and 47.8 %, respectively. In the groups given 5 and 10 mg/kg gRc, the frequency for the 200–600 μm^2 range was approximately 23.3 % and 24.5 %, respectively, while for the 600–2000 μm^2 range, it was about 76.7 % and 75.5 %. The group that received Rv showed a similar trend to the control group, with 18.4 % in the 200–600 μm^2 range and 81.7 % in the 600–2000 μm^2 range. As gRc and Rv protected against DEX-induced muscle atrophy, we examined their impact on muscle degradation-related proteins in muscle tissues. In mice treated with DEX, the levels of Atrogin-1 and MuRF1 were significantly higher than in control mice. The administration of gRc and Rv significantly reduced the expression of Atrogin-1 and MuRF1 (Fig. 5D and E). We then measured the LDH activity in serum, an indirect blood marker of muscle damage. In the DEX group, the level was significantly higher at 3601 mU/mL compared to the control group at 2126 mU/mL. Conversely, groups treated with gRc and Rv showed decreased levels similar to the control group (Fig. 5F). These findings show that gRc effectively reduces DEX-induced weight loss and muscle damage, lessens muscle atrophy, and preserves muscle function.

3.6. gRc binds to GR in molecular docking analysis

In a molecular docking, the binding affinity between DEX and GR was calculated to be −7.4 kcal/mol, and the binding affinity between gRc and GR was calculated to be −9.4 kcal/mol, indicating that the interaction potential of gRc is higher than that of DEX (Fig. 6). In the 3D secondary structure, both compounds were predicted to interact with the NF LBD at the same position. In particular, gRc interacts in a wider range than DEX, and included all two sites out of DEX binding site candidates (Supplementary Fig. S5). In the 2D diagram, it was confirmed that the two compounds were interacting at the amino acid sequence at position 585. On the 3D molecular surface, both compounds were observed to interact within the pore of the LBD region of GR. To strengthen our findings from the docking analysis, we conducted additional analyses to explore the interaction between gRc and the GR pathway. GSEA results show significant downregulation of the GR pathway by gRc treatment under DEX conditions (Supplementary Fig. S6A). Network analysis also identifies specific target genes within the GR pathway inhibited by gRc treatment (Supplementary Fig. S6B).

4. Discussion

Sarcopenia, the loss of muscle mass and strength, is prevalent in older adults and linked to aging, cancer, cardiovascular diseases, and specific medications [1–3,5]. Prolonged exposure to high levels of GC in skeletal muscle decreases protein synthesis and increases proteolysis, resulting in muscle atrophy [11]. Muscle atrophy triggers proteolytic systems that degrade contractile proteins in muscle tissue, leading to a decrease in muscle size. Several growth factors, like insulin-like growth factor-1 (IGF-1) and myostatin, regulate muscle development and play a role in the impact of GCs on muscle mass and function. Various nutrients, like omega-3 fatty acids, vitamins, and amino acids, can help prevent muscle atrophy caused by GC [14,15,24,38,39]. However,

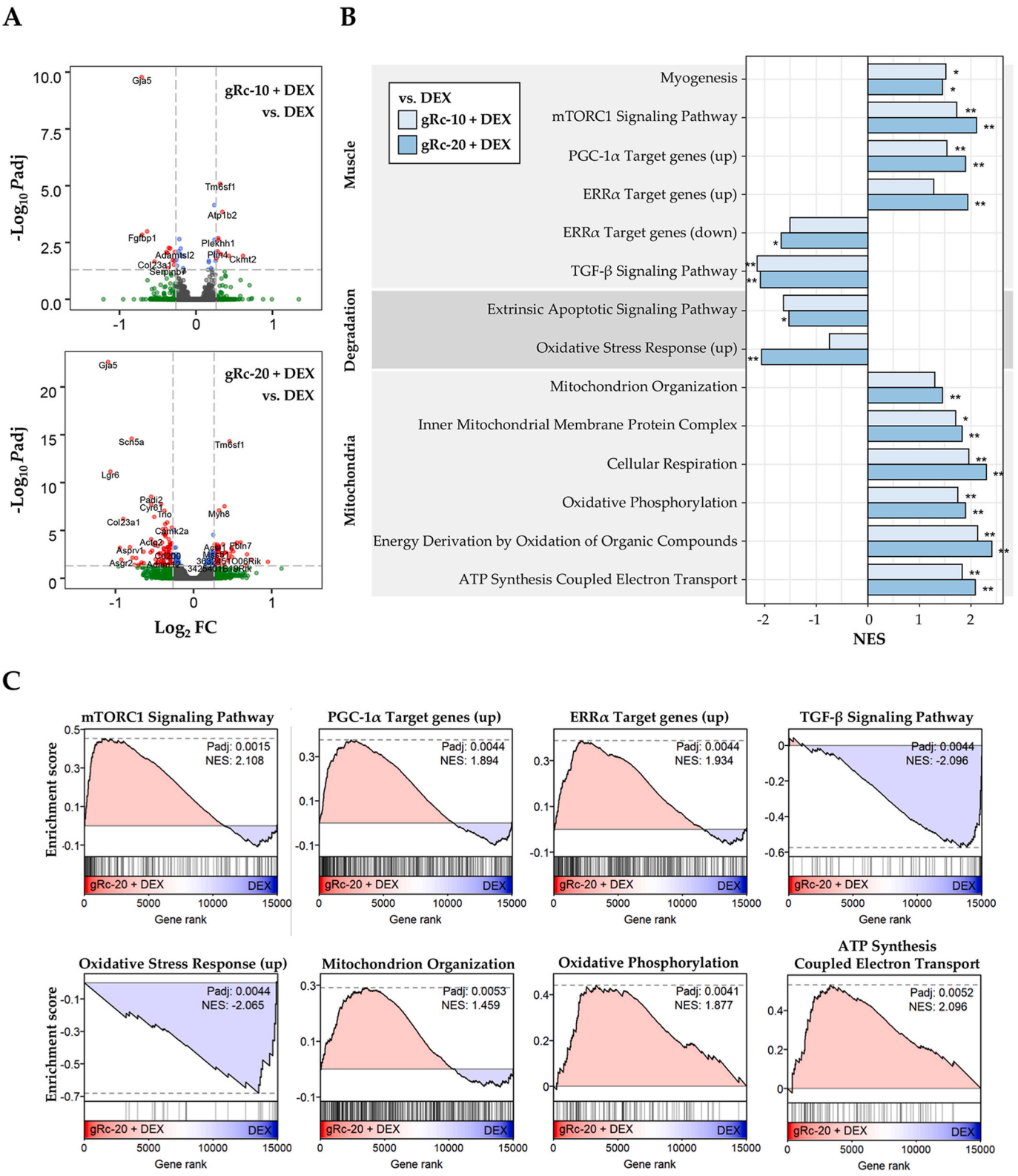

Fig. 3. Pathway analysis in C2C12 myotubes. (A) Differential gene expression analysis was conducted on transcriptome data from DEX-treated C2C12 myotubes with or without the pretreatments of gRc 10 μM (gRc-10) and 20 μM (gRc-20). Significance was determined by a fold-change (FC) of 1.2 and an adjusted *p*-value (Padj) of 0.05. (B) Gene set enrichment analysis (GSEA) highlighting enriched terms related to muscle generation, degradation, and mitochondrial function. (C) GSEA plots of enriched terms after pretreatments of gRc-20 in DEX-treated C2C12 myotubes. *, Padj <0.05; **, Padj <0.01; NES, normalized enrichment score.

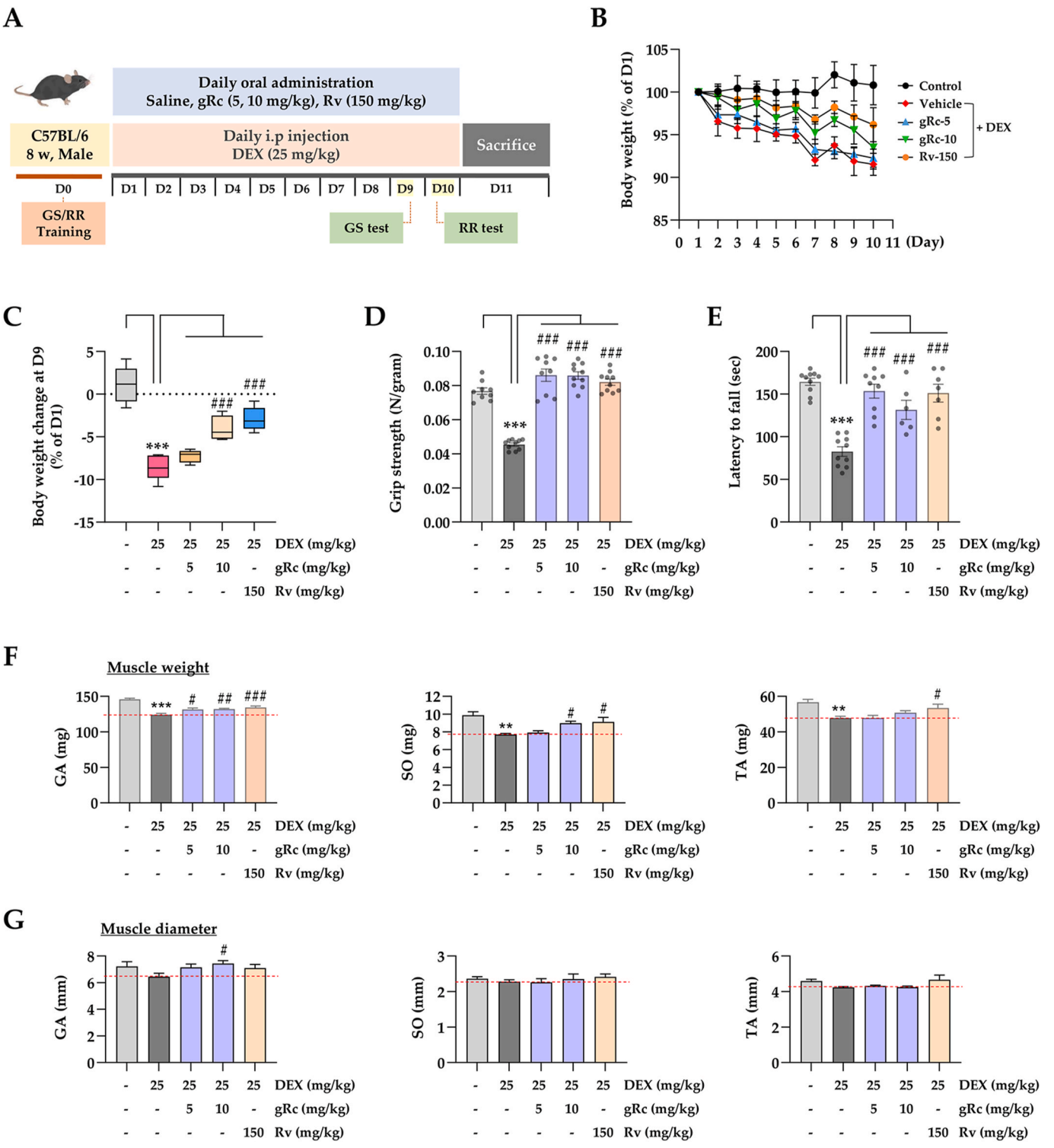

Fig. 4. Effects of gRc on muscle function and muscle mass in mice with DEX-induced muscle atrophy. (A) Scheme of the experiment. (B) The relative body weight compared to that of D1 was expressed as the means ± SEM (n = 10). (C) The final body weight change on D9 compared to the weight on D1 was presented as the means ± SEM (n = 10). (D) On D9, forelimb grip strength tests were performed. Grip strength was determined by dividing the force (N) by the body weight (grams) and expressed as the means ± SEM (n = 10). (E) On D10, the duration of time until falling off the rotarod apparatus was measured and expressed as the means ± SEM (n = 10). (F) The weight of GO, SO, and TA muscles were expressed as the means ± SEM (n = 10). (G) Muscle diameter was measured and expressed as the means ± SEM (n = 5). $^{**}p < 0.01$, $^{***}p < 0.001$ vs. vehicle-treated cells, $\#p < 0.05$, $\#\#p < 0.01$, $\#\#\#p < 0.001$ vs. DEX + vehicle-treated cells.

clarification is needed to develop clinically effective treatments for muscle atrophy induced by GC.

Exposure to DEX increases ROS production, causing mitochondrial dysfunction and muscle fiber degradation [7,11]. We consistently observed that DEX induced the breakdown of muscle proteins like MyHC and reduced mitochondrial mass in C2C12 myotubes. In a similar manner to the C2C12 *in vitro* model, DEX led to weight loss and decreased muscle fiber size and muscle function in the *in vivo* experimental mice. In both *in vitro* and *in vivo* model of DEX-induced muscle atrophy, Jakyak-gamcho-tang (JGT) counteracted the effects of DEX by

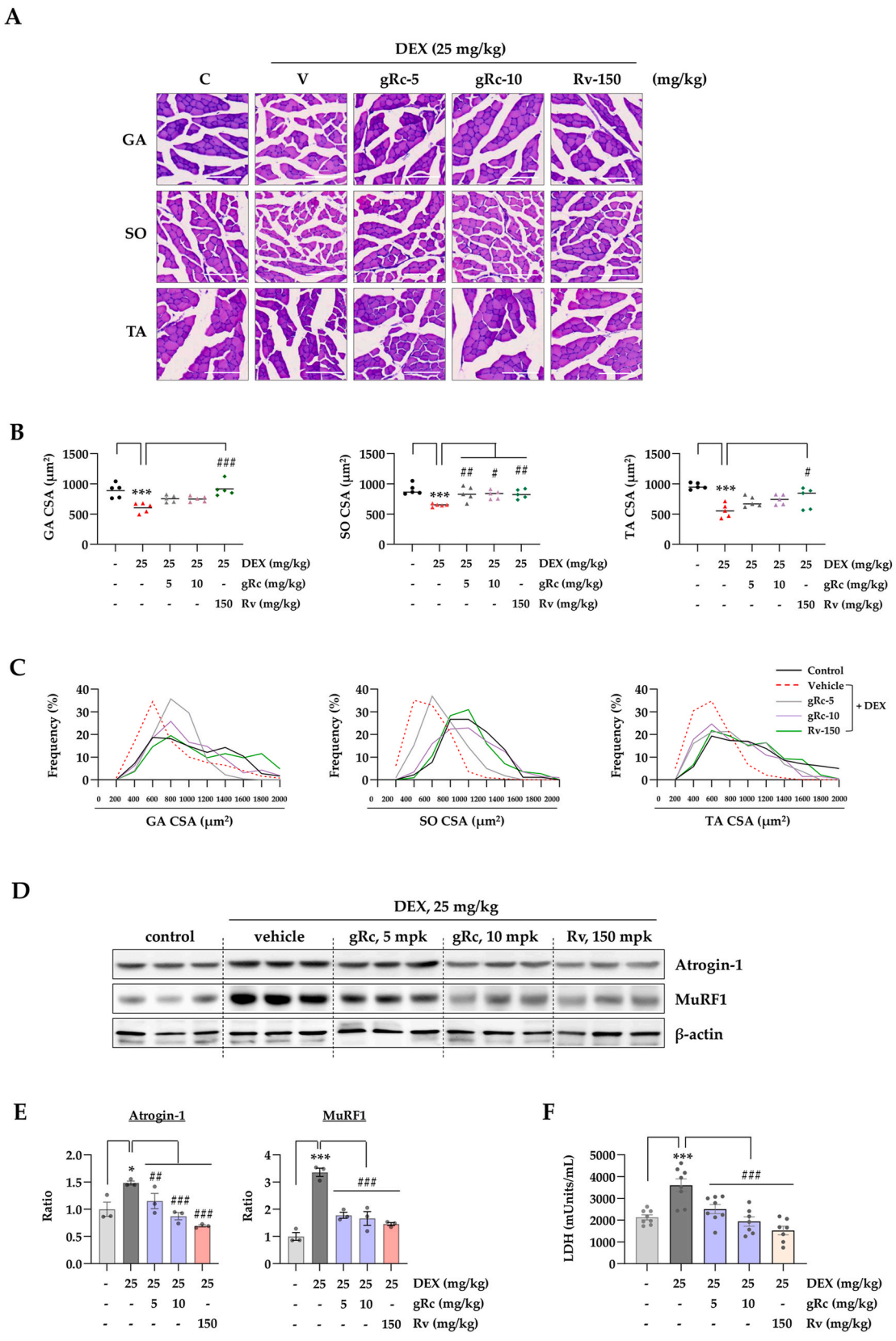

Fig. 5. Effects of gRc on myofibers and muscle degrading proteins in mice with DEX-induced muscle atrophy. (A) Images of cross-sectional myofibers were presented. Scale bar = 200 μm. (B) The CSA of muscle fibers was expressed as the means ± SEM (n = 5). (C) The frequency of CSA distribution was measured. (D–E) The protein levels of Atrogin-1 and MuRF1 in the TA muscles were determined by immunoblotting. Data are expressed as the means ± SEM (n = 3). (F) The LDH activity in sera are presented as the means ± SEM (n = 7–8). *$p < 0.05$, ***$p < 0.001$ vs. vehicle-treated cells, #$p < 0.05$, ##$p < 0.01$, ###$p < 0.001$ vs. DEX + vehicle-treated cells.

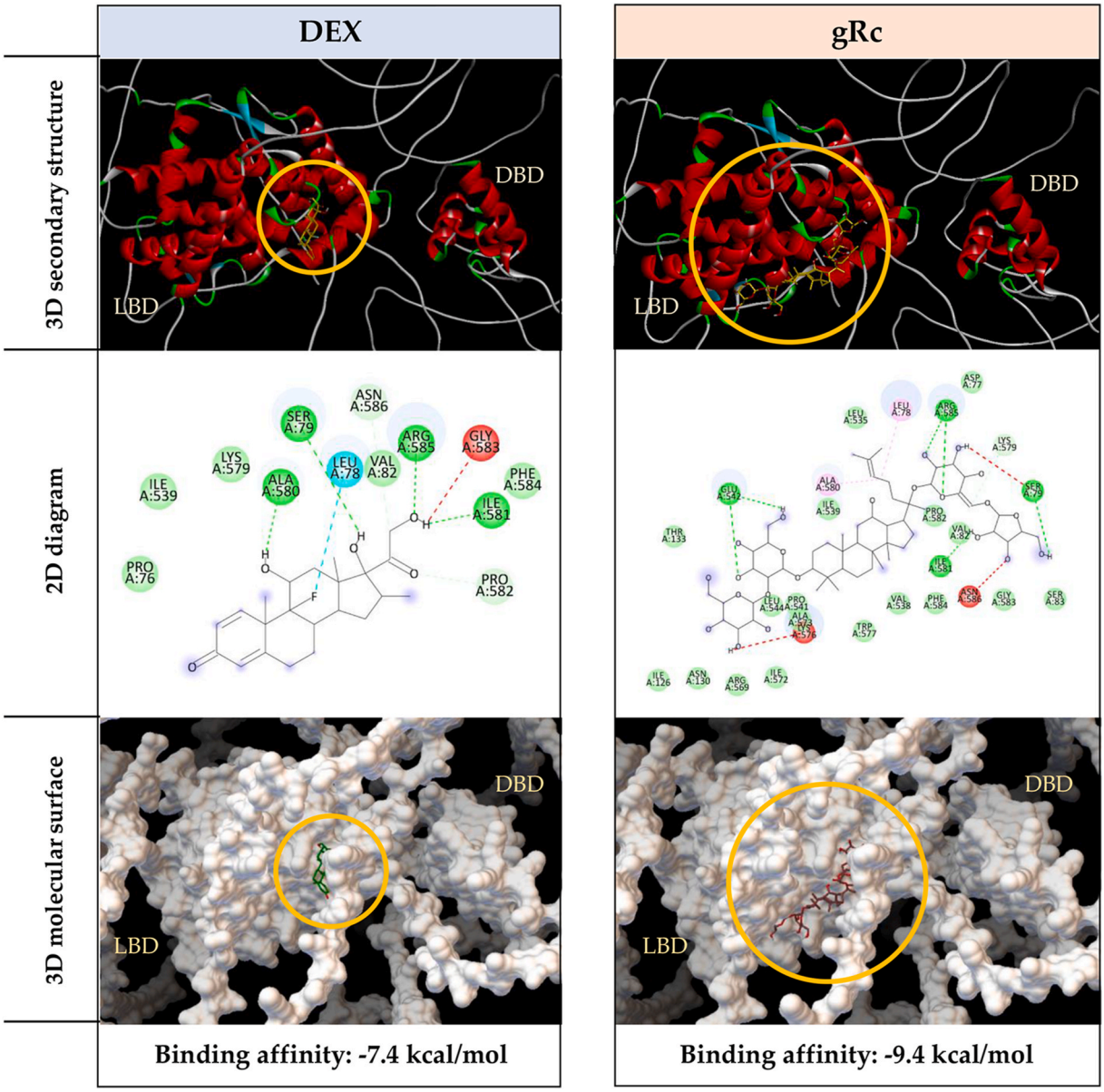

Fig. 6. Results of docking analysis on GR protein using DEX and gRc. The left column predicts the interaction between GR and DEX, while the right column predicts the interaction between GR and gRc. The structures can be visualized from the top in 3D secondary structure, 2D diagram, and 3D molecular surface. Yellow circles indicate the location where the compound interacts or the pore it interacts with. The ligand-binding domain (LBD) binds the ligand, and both compounds interact in this region.

preserving mitochondrial function, inhibiting muscle protein breakdown, and activating muscle-enhancing pathways. JGT enhances muscle strength and motor function, showing promise in preventing muscle atrophy caused by GC [25]. Additionally, it was reported that gRc protects muscle cells from oxidative stress and improves mitochondrial function by activating the PGC-1α pathway [23]. This research aimed to determine if gR can reduce DEX-induced muscle loss and weakness in both *in vitro* and *in vivo* muscle atrophy models.

This study showed that gRc effectively reduced the negative impact of DEX on both myoblasts and myotubes. In myotubes, the fusion index and tube length were maintained at levels similar to the normal group (Figs. 1 and 2). Transcriptome analysis of C2C12 myotubes revealed molecular mechanisms inversely regulated by gRc during DEX treatment, elucidating gRc's protective effects against DEX-induced muscle damage (Fig. 3). In a prior study, we analyzed muscle atrophy induced by H_2O_2 and DEX. H_2O_2 causes oxidative stress by generating ROS, damaging cells, while DEX affects cells by generating ROS and modulating pathways, leading to muscle atrophy [7,11,23]. We found limited overlap in pathways regulated by gRc between H_2O_2 and DEX conditions. (Supplementary Fig. S1A). However, common pathways modulated by gRc suggest consistent core mechanisms of muscle protection across conditions (Supplementary Figs. S1B and S1C). We discovered that gRc upregulates genes like *Ak4*, *BNIP3*, *Ckmt2*, and *Mb* in DEX-treated C2C12 myotubes (Supplementary Fig. S1). *Ak4*, encoding adenylate kinase 4, is involved in the mTORC1 signaling pathway, cellular respiration, and mitochondrial function. It helps reduce DEX-induced ROS and protects cells from oxidative stress [40]. *BNIP3*, associated with mitochondrial organization and energy production, has been shown to reduce muscle inflammation and atrophy [41]. *Ckmt2*, a target gene of ERRα and PGC-1α pathways, encodes mitochondrial creatine kinase, enhancing mitochondrial respiration [42]. *Mb*, encoding myoglobin, is essential for storing and transporting oxygen from the cell membrane to mitochondria. These genes, upregulated by gRc, may counteract the effects of DEX and help protect muscles. Additional

research is required to identify the main pathways through which gRc protects muscles against DEX, considering the various pathways involved in regulating muscle atrophy [43,44].

In an experimental mouse model, oral administration of 10 mg/kg gRc restored the body weight to a level similar to the positive control, Rv. gRc significantly improved muscle strength and exercise capacity that had been reduced by DEX, bringing them to levels similar to those of the control group. The administration of gRc effectively suppressed DEX-induced muscle atrophy, as confirmed by muscle cross-section analysis. Furthermore, gRc effectively reduced the LDH in blood and muscle breakdown proteins in muscle tissues (Figs. 4 and 5). The study showed the *in vivo* effectiveness of gRc in protecting against DEX-induced muscle damage. Finally, docking analysis was conducted on DEX, known to induce muscle atrophy by acting as a GR agonist, and gRc, which experimental results indicated prevents this. The analysis showed that gRc has a higher binding affinity than DEX at the same site (Fig. 6), suggesting gRc's potential as an antagonist and competitive inhibitor of DEX. This finding was supported by GSEA, indicating the downregulation of the GR pathway by gRc. However, it is important to note that these *in silico* analyses are not definitive. Biochemical assays, like the PolarScreen™ Glucocorticoid Receptor Competitor Assay Kit, are necessary to confirm the competitive inhibition hypothesis. Future research will combine these assays to comprehensively validate gRc's interaction with the GR pathway.

Our research suggests that gRc may protect against weight loss and muscle atrophy induced by DEX. This is accomplished by regulating molecular signals that aid in preserving muscle mass, reducing muscle protein breakdown, and enhancing muscle synthesis.

5. Conclusion

Overall, the findings suggest that gRc has broad protective effects in different stressful situations, showcasing its adaptability and potential therapeutic advantages for muscle-related disorders.

Data availability statement

The raw sequencing data (FASTQ files) and processed count data were uploaded to the Gene Expression Omnibus under the accession number GSE261787.

CRediT authorship contribution statement

Aeyung Kim: Conceptualization, Methodology, Investigation, Validation, Writing – original draft, Writing – review & editing, Funding acquisition. **Sang-Min Park:** Formal analysis, Writing – original draft, Writing – review & editing. **No Soo Kim:** Investigation, Validation, Writing – review & editing. **Musun Park:** Formal analysis, Data curation, Writing – original draft, Writing – review & editing. **Seongwon Cha:** Writing – review & editing, Funding acquisition, All authors have read and agreed to the published version of the manuscript.

Declaration of competing interest

The authors declare that they have no known competing financial interests or personal relationships that could have appeared to influence the work reported in this paper.

Acknowledgments

This work was supported by grant number KSN1722122 from the Korea Institute of Oriental Medicine (KIOM) and provided by National Research Foundation of Korea grants funded by the Korean Government (NRF-2020R1A2C1101602).

Appendix B. Supplementary data

Supplementary data to this article can be found online at https://doi.org/10.1016/j.jgr.2024.09.002.

References

[1] Sayer AA, Cruz-Jentoft A. Sarcopenia definition, diagnosis and treatment: consensus is growing. Age Ageing 2022;51. https://doi.org/10.1093/ageing/afac220.
[2] Cho MR, Lee S, Song SK. A review of sarcopenia pathophysiology, diagnosis, treatment and future direction. J Korean Med Sci 2022;37:e146. https://doi.org/10.3346/jkms.2022.37.e146.
[3] Marcell TJ. Sarcopenia: causes, consequences, and preventions. J Gerontol A Biol Sci Med Sci 2003;58:M911–6. https://doi.org/10.1093/gerona/58.10.m911.
[4] Xia L, Zhao R, Wan Q, Wu Y, Zhou Y, Wang Y, Cui Y, Shen X, Wu X. Sarcopenia and adverse health-related outcomes: an umbrella review of meta-analyses of observational studies. Cancer Med 2020;9:7964–78. https://doi.org/10.1002/cam4.3428.
[5] Larsson L, Degens H, Li M, Salviati L, Lee YI, Thompson W, Kirkland JL, Sandri M. Sarcopenia: aging-related loss of muscle mass and function. Physiol Rev 2019;99:427–511. https://doi.org/10.1152/physrev.00061.2017.
[6] Jang JY, Kim D, Kim ND. Pathogenesis, intervention, and current status of drug development for sarcopenia: a review. Biomedicines 2023;11. https://doi.org/10.3390/biomedicines11061635.
[7] Sato AY, Richardson D, Cregor M, Davis HM, Au ED, McAndrews K, Zimmers TA, Organ JM, Peacock M, Plotkin LI, et al. Glucocorticoids induce bone and muscle atrophy by tissue-specific mechanisms upstream of E3 ubiquitin ligases. Endocrinology 2017;158:664–77. https://doi.org/10.1210/en.2016-1779.
[8] Hardy RS, Raza K, Cooper MS. Therapeutic glucocorticoids: mechanisms of actions in rheumatic diseases. Nat Rev Rheumatol 2020;16:133–44. https://doi.org/10.1038/s41584-020-0371-y.
[9] van der Velden VH. Glucocorticoids: mechanisms of action and anti-inflammatory potential in asthma. Mediators Inflamm 1998;7:229–37. https://doi.org/10.1080/09629359890910.
[10] Ma K, Mallidis C, Bhasin S, Mahabadi V, Artaza J, Gonzalez-Cadavid N, Arias J, Salehian B. Glucocorticoid-induced skeletal muscle atrophy is associated with upregulation of myostatin gene expression. Am J Physiol Endocrinol Metab 2003;285:E363–71. https://doi.org/10.1152/ajpendo.00487.2002.
[11] Schakman O, Kalista S, Barbe C, Loumaye A, Thissen JP. Glucocorticoid-induced skeletal muscle atrophy. Int J Biochem Cell Biol 2013;45:2163–72. https://doi.org/10.1016/j.biocel.2013.05.036.
[12] Chen X, Ji Y, Liu R, Zhu X, Wang K, Yang X, Liu B, Gao Z, Huang Y, Shen Y, et al. Mitochondrial dysfunction: roles in skeletal muscle atrophy. J Transl Med 2023;21:503. https://doi.org/10.1186/s12967-023-04369-z.
[13] Agrawal S, Chakole S, Shetty N, Prasad R, Lohakare T, Wanjari M. Exploring the role of oxidative stress in skeletal muscle atrophy: mechanisms and implications. Cureus 2023;15:e42178. https://doi.org/10.7759/cureus.42178.
[14] Ulla A, Uchida T, Miki Y, Sugiura K, Higashitani A, Kobayashi T, Ohno A, Nakao R, Hirasaka K, Sakakibara I, et al. Morin attenuates dexamethasone-mediated oxidative stress and atrophy in mouse C2C12 skeletal myotubes. Arch Biochem Biophys 2021;704:108873. https://doi.org/10.1016/j.abb.2021.108873.
[15] Wang P, Kang SY, Kim SJ, Park YK, Jung HW. Monotropein improves dexamethasone-induced muscle atrophy via the AKT/mTOR/FOXO3a signaling pathways. Nutrients 2022;14. https://doi.org/10.3390/nu14091859.
[16] Hanada M, Sakamoto N, Ishimatsu Y, Kakugawa T, Obase Y, Kozu R, Senjyu H, Izumikawa K, Mukae H, Kohno S. Effect of long-term treatment with corticosteroids on skeletal muscle strength, functional exercise capacity and health status in patients with interstitial lung disease. Respirology 2016;21:1088–93. https://doi.org/10.1111/resp.12807.
[17] Leung KW, Wong AS. Pharmacology of ginsenosides: a literature review. Chin Med 2010;5:20. https://doi.org/10.1186/1749-8546-5-20.
[18] Ratan ZA, Haidere MF, Hong YH, Park SH, Lee JO, Lee J, Cho JY. Pharmacological potential of ginseng and its major component ginsenosides. J Ginseng Res 2021;45:199–210. https://doi.org/10.1016/j.jgr.2020.02.004.
[19] Lee CH, Kim JH. A review on the medicinal potentials of ginseng and ginsenosides on cardiovascular diseases. J Ginseng Res 2014;38:161–6. https://doi.org/10.1016/j.jgr.2014.03.001.
[20] Kim HJ, Kim P, Shin CY. A comprehensive review of the therapeutic and pharmacological effects of ginseng and ginsenosides in central nervous system. J Ginseng Res 2013;37:8–29. https://doi.org/10.5142/jgr.2013.37.8.
[21] Hong H, Baatar D, Hwang SG. Anticancer activities of ginsenosides, the main active components of ginseng. Evid Based Complement Alternat Med 2021;2021:8858006. https://doi.org/10.1155/2021/8858006.
[22] Zha W, Sun Y, Gong W, Li L, Kim W, Li H. Ginseng and ginsenosides: therapeutic potential for sarcopenia. Biomed Pharmacother 2022;156:113876. https://doi.org/10.1016/j.biopha.2022.113876.
[23] Kim A, Park SM, Kim NS, Lee H. Ginsenoside Rc, an active component of Panax ginseng, alleviates oxidative stress-induced muscle atrophy via improvement of mitochondrial biogenesis. Antioxidants 2023;12. https://doi.org/10.3390/antiox12081576.
[24] Wang L, Jiao XF, Wu C, Li XQ, Sun HX, Shen XY, Zhang KZ, Zhao C, Liu L, Wang M, et al. Trimetazidine attenuates dexamethasone-induced muscle atrophy via

inhibiting NLRP3/GSDMD pathway-mediated pyroptosis. Cell Death Discov 2021; 7:251. https://doi.org/10.1038/s41420-021-00648-0.
[25] Kim A, Kim YR, Park SM, Lee H, Park M, Yi JM, Cha S, Kim NS. Jakyak-gamcho-tang, a decoction of Paeoniae Radix and Glycyrrhizae Radix et Rhizoma, ameliorates dexamethasone-induced muscle atrophy and muscle dysfunction. Phytomedicine 2024;123:155057. https://doi.org/10.1016/j.phymed.2023.155057.
[26] Liu W, Han F, Qu S, Yao Y, Zhao J, Akhtar ML, Ci Y, Zhang H, Li H, Zhao Y, et al. MARVELD1 depletion leads to dysfunction of motor and cognition via regulating glia-dependent neuronal migration during brain development. Cell Death Dis 2018; 9:999. https://doi.org/10.1038/s41419-018-1027-6.
[27] Dobin A, Davis CA, Schlesinger F, Drenkow J, Zaleski C, Jha S, Batut P, Chaisson M, Gingeras TR. STAR: ultrafast universal RNA-seq aligner. Bioinformatics 2013;29: 15–21. https://doi.org/10.1093/bioinformatics/bts635.
[28] Li B, Dewey CN. RSEM: accurate transcript quantification from RNA-Seq data with or without a reference genome. BMC Bioinf 2011;12:323. https://doi.org/10.1186/1471-2105-12-323.
[29] Love MI, Huber W, Anders S. Moderated estimation of fold change and dispersion for RNA-seq data with DESeq2. Genome Biol 2014;15:550. https://doi.org/10.1186/s13059-014-0550-8.
[30] Subramanian A, Tamayo P, Mootha VK, Mukherjee S, Ebert BL, Gillette MA, Paulovich A, Pomeroy SL, Golub TR, Lander ES, et al. Gene set enrichment analysis: a knowledge-based approach for interpreting genome-wide expression profiles. Proc Natl Acad Sci U S A 2005;102:15545–50. https://doi.org/10.1073/pnas.0506580102.
[31] Kim S, Chen J, Cheng T, Gindulyte A, He J, He S, Li Q, Shoemaker BA, Thiessen PA, Yu B, et al. PubChem 2019 update: improved access to chemical data. Nucleic Acids Res 2019;47:D1102–9. https://doi.org/10.1093/nar/gky1033.
[32] Wishart DS, Guo A, Oler E, Wang F, Anjum A, Peters H, Dizon R, Sayeeda Z, Tian S, Lee BL, et al. Hmdb 5.0: the human Metabolome database for 2022. Nucleic Acids Res 2022;50:D622–31. https://doi.org/10.1093/nar/gkab1062.
[33] UniProt C. UniProt: a worldwide hub of protein knowledge. Nucleic Acids Res 2019;47:D506–15. https://doi.org/10.1093/nar/gky1049.
[34] Varadi M, Anyango S, Deshpande M, Nair S, Natassia C, Yordanova G, Yuan D, Stroe O, Wood G, Laydon A, et al. AlphaFold Protein Structure Database: massively expanding the structural coverage of protein-sequence space with high-accuracy models. Nucleic Acids Res 2022;50:D439–44. https://doi.org/10.1093/nar/gkab1061.
[35] O'Boyle NM, Banck M, James CA, Morley C, Vandermeersch T, Hutchison GR. Open Babel: an open chemical toolbox. J Cheminform 2011;3:33. https://doi.org/10.1186/1758-2946-3-33.
[36] Trott O, Olson AJ. AutoDock Vina: improving the speed and accuracy of docking with a new scoring function, efficient optimization, and multithreading. J Comput Chem 2010;31:455–61. https://doi.org/10.1002/jcc.21334.
[37] Gan M, Ma J, Chen J, Chen L, Zhang S, Zhao Y, Niu L, Li X, Zhu L, Shen L. miR-222 is involved in the amelioration effect of genistein on dexamethasone-induced skeletal muscle atrophy. Nutrients 2022;14. https://doi.org/10.3390/nu14091861.
[38] Duan Y, Zhong Y, Song B, Zheng C, Xu K, Kong X, Li F. Suppression of protein degradation by leucine requires its conversion to beta-hydroxy-beta-methyl butyrate in C2C12 myotubes. Aging (Albany NY) 2019;11:11922–36. https://doi.org/10.18632/aging.102509.
[39] Di Cesare Mannelli L, Micheli L, Lucarini E, Parisio C, Toti A, Tenci B, Zanardelli M, Branca JJV, Pacini A, Ghelardini C. Effects of the combination of beta-Hydroxy-beta-Methyl butyrate and R(+) lipoic acid in a cellular model of sarcopenia. Molecules 2020;25. https://doi.org/10.3390/molecules25092117.
[40] Fujisawa K, Terai S, Takami T, Yamamoto N, Yamasaki T, Matsumoto T, Yamaguchi K, Owada Y, Nishina H, Noma T, et al. Modulation of anti-cancer drug sensitivity through the regulation of mitochondrial activity by adenylate kinase 4. J Exp Clin Cancer Res 2016;35:48. https://doi.org/10.1186/s13046-016-0322-2.
[41] Irazoki A, Martinez-Vicente M, Aparicio P, Aris C, Alibakhshi E, Rubio-Valera M, Castellanos J, Lores L, Palacin M, Guma A, et al. Coordination of mitochondrial and lysosomal homeostasis mitigates inflammation and muscle atrophy during aging. Aging Cell 2022;21:e13583. https://doi.org/10.1111/acel.13583.
[42] Rizo-Roca D, Guimaraes DS, Pendergrast LA, Di Leo N, Chibalin AV, Maqdasy S, Ryden M, Naslund E, Zierath JR, Krook A. Decreased sarcomeric mitochondrial creatine kinase 2 impairs skeletal muscle mitochondrial function independently of insulin action in type 2 diabetes. bioRxiv 2024;2024:2001–11. 575194.
[43] Cho S, Lee H, Lee HY, Kim SJ, Song W. The effect of fibroblast growth factor receptor inhibition on resistance exercise training-induced adaptation of bone and muscle quality in mice. KOREAN J PHYSIOL PHARMACOL 2022;26:207–18. https://doi.org/10.4196/kjpp.2022.26.3.207.
[44] Yin L, Li N, Jia W, Wang N, Liang M, Yang X, Du G. Skeletal muscle atrophy: from mechanisms to treatments. Pharmacol Res 2021;172:105807. https://doi.org/10.1016/j.phrs.2021.105807.